

# Magnetophoretic-based microfluidic device for DNA Concentration

Sangjo Shim<sup>1,2,3</sup> · Jiwook Shim<sup>1,2</sup> · William R. Taylor<sup>4,5</sup> · Farhad Kosari<sup>4,5</sup> · George Vasmatzis<sup>4,5</sup> · David A. Ahlquist<sup>4,5</sup> · Rashid Bashir<sup>1,2,3,5</sup>

© Springer Science+Business Media New York 2016

**Abstract** Nucleic acids serve as biomarkers of disease and it is highly desirable to develop approaches to extract small number of such genomic extracts from human bodily fluids. Magnetic particles-based nucleic acid extraction is widely used for concentration of small amount of samples and is followed by DNA amplification in specific assays. However, approaches to integrate such magnetic particles based capture with micro and nanofluidic based assays are still lacking. In this report, we demonstrate a magnetophoretic-based approach for target-specific DNA extraction and concentration within a microfluidic device. This device features a large chamber for reducing flow velocity and an array of  $\mu$ -magnets for enhancing magnetic flux density. With this strategy, the device is able to collect up to 95 % of the magnetic particles from the fluidic flow and to concentrate these magnetic particles in a collection region. Then an enzymatic reaction is used to detach the DNA from the magnetic particles

within the microfluidic device, making the DNA available for subsequent analysis. Concentrations of over 1000-fold for 90 bp dsDNA molecules is demonstrated. This strategy can bridge the gap between detection of low concentration analytes from clinical samples and a range of micro and nanofluidic sensors and devices including nanopores, nanocantilevers, and nanowires.

**Keywords** Magnetophoresis · DNA concentration · DNA conjugated magnetic particles · Uracil linker · Uracil-specific excision reagent enzyme

## 1 Introduction

Serving as biomarkers of diseases or risks, a patient's genomic extracts can indicate probability and state of diseases as such as cancer (Das and Singal 2004; Laird 2003). DNA based diagnostics often uses PCR, ELISA and fluorescence hybridization and these approaches require isolation and purification of DNA for analysis (Kiiantsa and Maizels 2014; Nagy et al. 2005; Sirdah 2014). However, conventional methods for nucleic acids extraction are not suitable for low volume of genomic extracts from human bodily fluids (Mariella 2008; Niemz et al. 2011). For small number of DNA molecules, magnetic particles-based DNA separation methods have been developed and widely used (Sasso et al. 2012; Wu et al. 2010). Nevertheless, most conventional magnetic particles-based DNA collection methods require multiple steps of mixing magnetic particles with large volume of clinical sample containing precipitated DNA, washing, recollecting, eluting DNA, and re-suspending in final solution, before the target DNA is amplified (Azimi et al. 2011; Wu et al. 2010). Specifically, the level of methylated DNA obtainable from bodily fluids for detection of disease can be extremely low

**Electronic supplementary material** The online version of this article (doi:10.1007/s10544-016-0051-5) contains supplementary material, which is available to authorized users.

✉ Rashid Bashir  
rbashir@illinois.edu

<sup>1</sup> Department of Bioengineering, University of Illinois at Urbana-Champaign, Urbana, IL 61801, USA

<sup>2</sup> Micro and Nanotechnology Laboratory, University of Illinois at Urbana-Champaign, Urbana, IL 61801, USA

<sup>3</sup> Beckman Institute for Advanced Science and Technology, University of Illinois at Urbana-Champaign, Urbana, IL 61801, USA

<sup>4</sup> Department of Molecular Medicine, Center for Individualized Medicine, Mayo Clinic, Rochester, MN 55905, USA

<sup>5</sup> Mayo-Illinois Alliance for Technology Based Healthcare, <http://www.mayoillinois.org>

(Jahr et al. 2001), and the detection of DNA methylation requires bisulfite conversion that degrades DNA significantly during the process and thus could compromise detection results (Murrell et al. 2005).

In the recent past, we have developed methods for detection of DNA methylation using solid-state nanopores. Methylation sites on dsDNA were selectively labeled with proteins with methyl-binding domains, and the nanopore-based assay selectively detected the methylated DNA-protein complex with relative deeper and prolonged nanopore ionic current signatures compared to naked DNA (Shim et al. 2013; Shim et al. 2015). But the integration of such nanopore sensors with clinical samples requires capture and concentration of the target genomic DNA molecules from body fluids. The genomic DNA can be readily obtained from human bodily fluids such as serum, plasma, urine, and stool samples (Kandimalla et al. 2013; Kisiel et al. 2012; Laird 2003; Zou et al. 2009). Further, the feasibility of cancer detection by analyzing epigenetic patterns, and aberrant DNA methylation on genomic extracts from bodily fluids has been previously reported (Laird 2003). For these applications and to be used in conjunction with nanopore sensors for DNA methylation, a new method is needed that can result in the concentration of sequence-specific DNA close to the sensor. In this report, we demonstrate a nucleic acids extraction method that is compatible with microfluidic and nanosensors-based detection of DNA. We demonstrate  $\mu$ -magnet integrated microfluidic device for concentration of target-specific nucleic acids. This method could be applicable for use with clinical samples in microfluidic lab on chip devices and especially nanopore and nanochannel based sensing approaches.

## 2 Results and discussion

### 2.1 DNA attachment to magnetic particles

To selectively capture target DNA, sequence-specific complementary DNA was designed along with addition of four uracil bases, a twelve-carbon spacer, and an amine at the 5' end. The four uracil bases were added to later detach the DNA from magnetic particles by enzymatic reaction using uracil-specific excision reagent. The twelve-carbon spacer was added to allow enough room for the enzymes to access the four uracil bases. Schematic shows DNA-magnetic particles conjugation and detachment of DNA from magnetic particles (Fig 1a). Carboxylated magnetic particles were obtained (see the materials and methods section) and resuspended at final concentration of 22.2 pM (corresponding to  $1 \times$  magnetic particles) in  $1 \times$  Tris-EDTA solution. The complementary DNA was mixed with the  $0.5 \times$  Saline-Sodium Citrate (SSC) solution to capture the target DNA in a micro-centrifuge tube (see the materials and methods section). The DNA-magnetic particles

conjugation was formed through carboxyl-amine crosslinking as indicated in instructions given from manufacturer. After capturing the target DNA, the magnetic particles were recollected at the bottom of the tube using magnets, and supernatant was gently collected to measure the amount of unbound target DNA using qPCR. DNA, Primers and probe are carefully designed to avoid any possible secondary and tertiary structures (<sup>‡</sup>See Supplementary Information, Fig. S1). Figure 1b shows the recovery of quantified unbound DNA after DNA-magnetic particles conjugation, showing high yield of conjugation ratio at various DNA and particle concentration. We show that more than 97 % of DNA is conjugated to magnetic particles at concentration of 1.67 nM DNA and 221.67 pM magnetic particles. After gently removing the supernatant, 1  $\mu$ l of  $20 \times$  USER enzyme was added to the 20  $\mu$ l of magnetic particles pellet remained in the tube. The tube was stored at the room temperature ( $24 \pm 2$  °C) for 30 min without any agitation. The double-stranded DNA was detached from magnetic particles using uracil-specific excision reagent (USER) enzyme that contains uracil-DNA glycosylase (UDG) and DNA glycosylase-lyse endonuclease VIII. Compared to other DNA detaching method, enzymatic reaction method does not require elution (Azimi et al. 2011). Consequently, DNA remains in double-stranded form and in concentrated conditions. The concentrated dsDNA could then be coupled with various DNA methylation measurement assays using electrical measurement or fluorescent optical measurement (Cerf et al. 2011; Shim et al. 2013; Shim et al. 2015). The detached DNA was gently collected and quantified using qPCR (<sup>‡</sup>See Supplementary Information, Fig. S2). The detachment of DNA was tested at various ratios between DNA conjugated magnetic particles and USER enzyme, more than 90 % of DNA was recovered when  $1.3 \times 10^5$  of magnetic particles in 1  $\mu$ l is mixed with  $6.6 \times 10^6$  molecules of USER enzymes in 1  $\mu$ l (Fig 1c). In addition, we have repeated the entire DNA-magnetic particles coupling and decoupling with single-stranded complementary DNA without capturing target DNA. The detachment rate by USER enzyme was very low and in the range of 1.8 % and 3.5 % while having high conjugation rate of over 99 % with magnetic particles. A possible reason for the low detachment is that EDAC, which is the coupling activator between carboxyl and amine, produces tertiary structure of ssDNA (Sheehan et al. 1961). The tertiary structure of ssDNA can prevent the USER enzyme reaching and cleaving the Uracils.

### 2.2 Magnetophoretic-based microfluidic device

In spite of recent reports such as the control of magnetotactic bacteria using integrated nanofabricated metallic islands (Gonzalez et al. 2014) and microfluidic magnetophoretic separation of rare mammalian cells (Forbes and Forry 2012), technique for in-situ biomolecules collection and

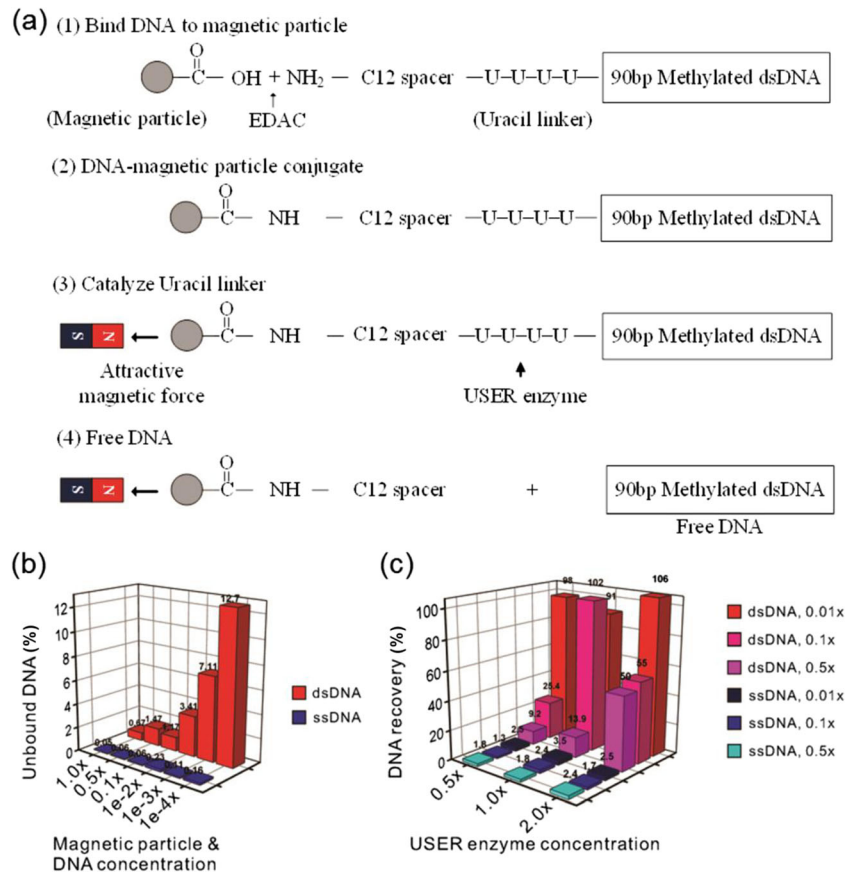


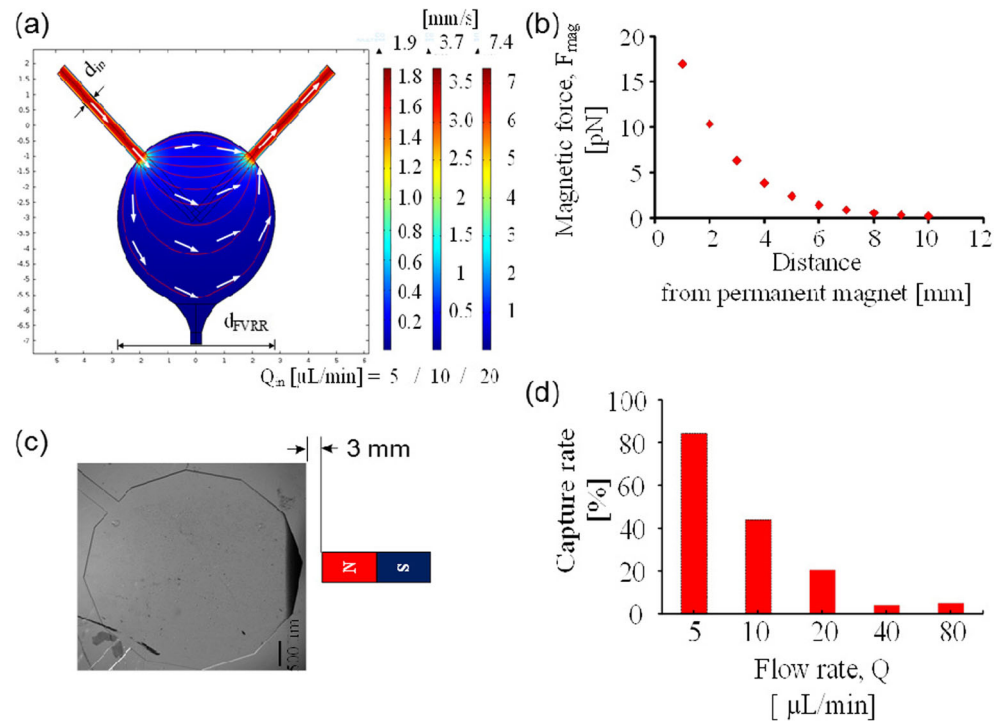
**Fig. 1** Conjugation and detachment between Methylated DNA and magnetic particles. **a-1** EDAC activated carboxyl-amine bonding between surface of carboxylated particles and amine group at terminal of C12 spacer. **a-2** The carboxyl-amine bond conjugated DNA to the particle. **a-3** A USER enzyme was introduced to the conjugation to cleave the four Uracils. **a-4** DNA was released from the particle after enzymatic reaction. **b** After conjugation between DNA and magnetic particles, DNA-conjugated particles were collected at the bottom of tube

using a magnet and then the supernatant was collected for quantification of unbound DNA using qPCR. The quantification result, showing a low density of unbound DNA, indicated that most DNA was successfully conjugated to the particles. **c** Enzymatic reaction to detach DNA from beads was tested at various concentrations between USER enzymes and DNA-conjugated beads. A high recovery was obtained from dsDNA while ssDNA showed extremely low recovery. (Supplementary Information Table S1 for concentration x in Fig. 1b and 1c)

concentration on the same chip are still needed for sample collection to high throughput sensing. In this work, magnetophoresis was utilized in microfluidic devices for magnetic particles collection and DNA concentration. Initially, microfluidic channels were fabricated to have simple V shape using conventional photolithography and PDMS fabrication techniques. The 100 μm channel width and 40 μm of channel height were chosen to provide enough space for magnetic particles to flow in the channel. A chamber of 360 μm diameter was fabricated to be slightly larger than the channel width for collection of magnetic particles at the bottom corner of V shape. A Neodymium magnet (BX084PC-WHT, K&J Magnetics), which is known for strong magnetic field at low mass, was placed at 8 mm from the bottom of the chamber to gently control the motion of magnetic particles in microfluidic flow (As shown in Fig. 2c but the distance between the magnet and the microfluidic device is 8 mm). The plain magnetic particles were prepared at final concentration of 2.22 pM in 1×

Tris-EDTA solution, and 200 μl of the magnetic particles solution was injected into the microfluidic channel at a constant fluidic flow using 1 ml syringe mounted on a syringe pump (see the materials and methods). The flow rate of 1.5 mm/s was set to complete injection of 200 μl in an hour. Despite the strong magnetic field, most magnetic particles escaped to the outlet channel with the fluidic flow rather than captured in the chamber (Supplementary Information, Fig. S3). Increase of the chamber size was needed to reduce the flow velocity for controlling of the magnetic particles motion with magnet. Flow velocity depending on chamber size was calculated and simulated using COMSOL with equation of  $V_{chamber} \approx (d_{in}/d_{chamber}) \cdot V_{in}$ , where  $V_{chamber}$  represents flow velocity in chamber,  $d_{in}$  for width of inlet channel,  $d_{chamber}$  for width of chamber, and  $V_{in}$  for flow velocity in inlet channel. COMSOL results (Fig. 2a) shows that flow velocity in the chamber can be reduced 15-fold at ~0.1 mm/s when the diameter of chamber is enlarged to 5.6 mm.

**Fig. 2** Simulation and experiment of magnetic particle concentration using magnetophoretic-based microfluidic device. **a** COMSOL multiphysics simulation shows the reduced flow velocity in the chamber. The flow rate of 1.5 mm/s at the input channel drops to 0.1 mm/s in the chamber. **b** The derived magnetic force decreases exponentially as a function of distance from the front permanent magnet. **c** The image shows capturing of particles in a magnetophoretic-based microfluidic device without the array of  $\mu$ -magnets. **d** The capturing of particles was demonstrated at 85 % at the flow rate of 5  $\mu$ L/min



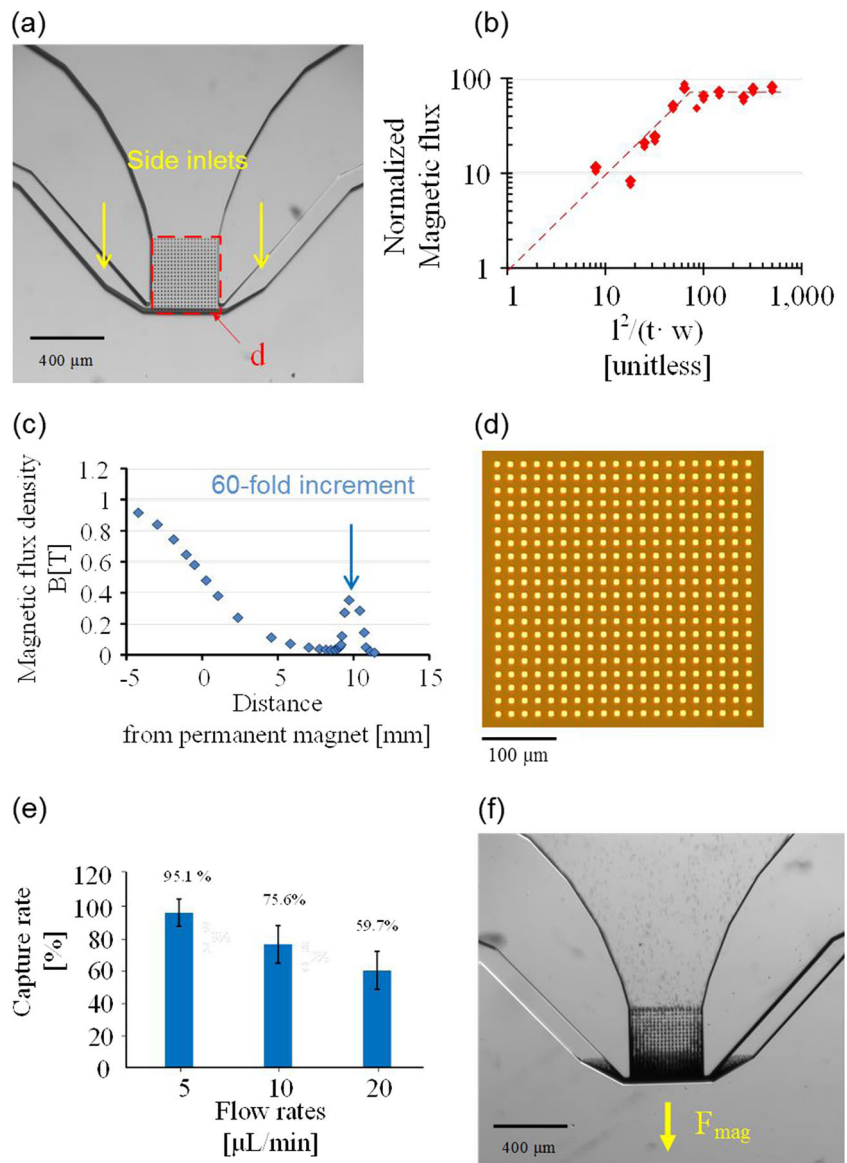
The distance between chamber and magnet was carefully chosen for optimal magnetic flux density, as magnetic force decreases exponentially with distance. The neodymium magnet that we used in this experiment has a magnetic flux density of 1.32 T. The magnetic force versus distance is plotted in Fig. 2b. Magnetic force was calculated using  $F_{mag-p} = \Delta\chi \cdot V_p \cdot \nabla (B^2/2\mu_0)$ , where  $\Delta\chi$  is the relative susceptibility of the magnetic particle,  $V_p$  is the volume of a single magnetic particle,  $B$  is the magnetic flux density, and  $\mu_0$  is the magnetic permeability constant. The distance was set at 3 mm to have sufficient magnetic force capturing and holding magnetic particles in the microfluidic flow. An image of magnetic particles collection at the bottom of the chamber using a magnetophoretic-based microfluidic device is shown in Fig. 2c. To measure the magnetic particle collection rate, the magnet was moved away from the chamber and the entire chamber was flushed with  $1\times$  Tris-EDTA solution. The number of magnetic particles in flushed solution was counted using flow cytometry. The magnetic particle capture rate at various fluidic flow velocities is shown in Fig. 2d. The magnetic particles capture rate increased up to 82 % with flow velocity reduction when the fluid was injected at the same velocity used in <sup>†</sup>Supplementary Information, Fig. S3.

The final microfluidic device was equipped with two additional functions (Fig. 3a); (i) Two side inlets were connected to the bottom of the chamber for efficient delivery of USER enzymes directly to the DNA conjugated

magnetic particles, and (ii) An array of  $\mu$ -scale magnetic flux density enhancer ( $\mu$ -magnets) was added at the magnetic particle collection region. The  $\mu$ -magnets enhance the magnetic flux density in the chamber, thus enabling the capture of more magnetic particles. As the magnetic particles are captured by the  $\mu$ -magnets, the subsequent injection of USER enzymes through the side inlets would not remove the magnetic particles out of the collection region. Also, as each  $\mu$ -magnet in the array attracts magnetic particles in the collection region, the magnetic particles are spread over the array, which also helps to allow the USER enzyme to reach the magnetic particles and increase the DNA recovery rate from the magnetic particles. To determine the size of the  $\mu$ -magnets, the magnetic flux density was calculated as  $B = \mu_0 \cdot (H + M)$ , where  $H$  is the magnetic field strength, and  $M$  is the magnetization, and  $\mu_0$  is the magnetic permeability constant,  $4\pi \times 10^{-7}$  [N/A<sup>2</sup>]. However, the magnetization is also accompanied with demagnetization in the opposite magnetic field direction. Demagnetization is expressed as  $H_d = -N_M \cdot M$ , where  $N_M$  is demagnetization factor. A shape-induced demagnetization factor for a prolate ellipsoid was reported, and  $N_M$  was determined by the difference between longest length and shortest length (Osborn 1945). The side aligned with magnetization direction is denoted as  $l$ , the side perpendicular to the magnetization direction is denoted as  $w$ , and the thickness of  $\mu$ -magnets is denoted as  $t$ . The various side lengths in a range of 10 and 100 were simulated using COMSOL, and approximately 10- to 60-fold enhancement



**Fig. 3** The integration of the  $\mu$ -magnets array into magnetophoretic-based microfluidic device. **a** The image shows the integrated  $\mu$ -magnets array in the magnetic particle collection region at the bottom of the chamber. **b** Simulation of normalized magnetic flux density. The dashed line is superimposed to show the saturation of the magnetic flux density. **c** The COMSOL simulation shows the enhanced magnetic flux density on the  $\mu$ -magnet at the distance of 10 mm from the permanent magnet. **d** . The optical microscopy image shows the array of  $20 \times 20$   $\mu$ -magnet in square shape of  $10 \mu\text{m} \times 10 \mu\text{m}$ . **e** The rate of magnetic particle collection increases to 95 % with the  $\mu$ -magnets array. **f** The magnetic particles are widely distributed over the  $\mu$ -magnets array



of magnetic flux density was obtained (Fig. 3b). The maximum enhancement of magnetic flux density is generated when the shape factor,  $l^2/(w \cdot t)$ , reaches 100 and above. The dimension of final  $\mu$ -magnets was chosen at  $l = 10 \mu\text{m}$ ,  $w = 10 \mu\text{m}$ , and  $t = 0.1 \mu\text{m}$  to have shape factor of 100, and the simulation showed 60-fold increment of magnetic flux density (Fig. 3c). An array of  $20 \times 20$   $\mu$ -magnets with these dimensions was fabricated in the particles collection region (Fig. 3d). The rate of magnetic particles collection was improved from 85 % without the  $\mu$ -magnets to up to 95 % with the  $\mu$ -magnets at 5  $\mu\text{L}/\text{min}$  of flow velocity (Fig. 3e). In addition, the magnetic particles were spatially distributed over the array of  $\mu$ -magnets as shown in Fig. 3f and Supplementary Information Fig. S4. The wide distribution of particles accommodates USER enzymes to reach particles more uniformly.

### 2.3 Collection and concentration of DNA

DNA conjugated magnetic particles were prepared and injected into the  $\mu$ -magnets integrated magnetophoretic-based microfluidic device using methods described above (for more information, see <sup>‡</sup>Supplementary Information, Fig. S5). After capturing the magnetic particles, fluidic flow through the inlet was stopped for 5 min at room temperature ( $24 \pm 2 \text{ }^\circ\text{C}$ ) to collect the slow moving magnetic particles. Then, in order to detach DNA from the magnetic particles, the USER enzymes were delivered to the collection of DNA conjugated magnetic particles through side inlets. The device was kept at room temperature for 30 min for completion of the enzymatic reaction. Providing no direct measurement of DNA concentration in the collection region, solution containing DNA was recollected out of the device for the

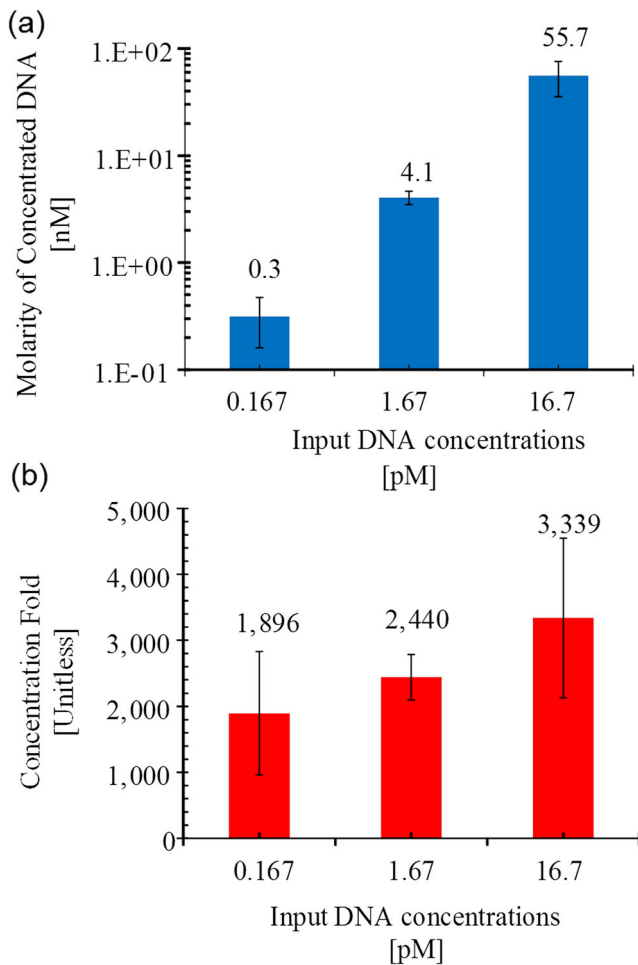


**Fig. 4** The result of collecting and concentrating DNA using the  $\mu$ -magnets integrated magnetophoretic-based microfluidic device. **a** The input DNA at the concentration of 0.167, 1.67, and 16.7 [pM] were concentrated to 0.3, 4.1, and 55.7 [nM] in the collection region. **b** The concentrated DNA at the collection region was 1000 to 3000-fold concentration compared to the initial DNA concentration

concentration measurement. The detached DNA in magnetic particle collection region was gently flushed through outlet channel using 500  $\mu$ l of 1 $\times$  Tris-EDTA solution. The DNA concentration in the magnetic particles collection region was calculated as  $M_{\text{con}} = (V_{\text{out}}/V_{\text{con}}) \cdot M_{\text{out}}$ , where  $M_{\text{con}}$  and  $M_{\text{out}}$  are concentrations of magnetic particles in the collection region and flushing solution, respectively, and  $V_{\text{con}}$  and  $V_{\text{out}}$  are volumes of magnetic particles collection region and flushing solution, respectively. Quantification of flushed DNA was performed using qPCR as described earlier in this report (see <sup>†</sup>Supplementary information, Fig. S2). The collection region volume of 22.4 nl was used to calculate the DNA concentrations, which were increased to 0.3 nM from 0.167 pM, 4.1 nM from 1.67 pM, and 55.7 nM from 16.7 pM (Fig. 4a). Hence, the DNA was concentrated over 1000-fold using the  $\mu$ -magnet integrated magnetophoretic-based microfluidic device (Fig. 4b).

### 3 Conclusion

A magnetophoretic-based microfluidic device integrated with  $\mu$ -magnets is developed for specific capture, collection, and concentration of target DNA. Complementary DNA is designed to capture target-specific DNA on magnetic particles, which are collected and concentrated using the device. The device features magnetics on chip to collect magnetic beads, enhancement of magnetic flux density, and detachment of DNA using enzymatic reactions. The entire processing takes about an hour to complete with 90 % of DNA recovery from the samples. The  $\mu$ -magnet integrated magnetophoretic-based microfluidic device demonstrates simplified processing steps and DNA concentration of over a 1000-fold. The results show feasibility of using pM range concentration of genomic extracts can be collected and concentrated to the level directly applicable for the-state-of-art micro and nanosensor assays on a chip. The concentrated double-stranded genomic extracts are good candidate for methylation assay using protein labeling (Shim et al. 2013; Shim et al. 2015).

### 4 Materials and methods

#### 1) Materials and sample preparation

##### A. Microfluidic channel fabrication

Microfluidic channels were microfabricated by conventional photolithography and PDMS techniques. The SU-8 (MicroChem, MA, USA) was coated on a clean silicon wafer in two steps, 500 rpm for 10 seconds and 1000 rpm for 30 seconds. The SU-8 coated silicon wafer was pre-baked at 65  $^{\circ}$ C for 10 min, then soft-baked at 95  $^{\circ}$ C for 30 min on a hotplate, and followed by cooling for 5 min. The SU-8 coated silicon wafer was exposed to UV (350–400 nm) at a dose of 480 mJ/cm<sup>2</sup> of EVG 620 mask aligner (EVG, NY, USA), and followed by a two-step post-expose-bake at 65  $^{\circ}$ C for 1 min and 95  $^{\circ}$ C for 10 min on a hotplate. After cooling down to the room temperature, the wafer was soaked in SU-8 developer solution and placed on the shaker for 15 min to develop patterns. The developed patterns were then rinsed with isopropyl alcohol (IPA) and dried gently with nitrogen. Dow Corning Sylgard 184 Silicone Elastomer (Ellsworth, WI, USA) was mixed with a curing agent at the weight ratio of 10: 1, degassed in a vacuum desiccator, and poured on the SU-8 mold, which was cleaned and coated with 3-mercaptopropyl trimethoxy silane in a vacuum desiccator for at least 30 min. The PDMS on the SU-8 mold was placed in an oven at 65  $^{\circ}$ C overnight. The cured PDMS master with microchannels was gently peeled off

from the mold, and inlet and outlet holes were made using a biopsy punch.

#### B. $\mu$ -magnet deposition on glass wafer

A borofloat 33 glass wafer (4-inch, University wafer, MA, USA) was cleaned using the piranha clean (sulfuric acid: hydrogen peroxide =1: 1). The entire glass wafer was spin-coated with the LOR 3 A (MicroChem, MA, USA) with two steps, 500 rpm for 2 seconds and 3000 rpm for 35 seconds, and followed by soft bake at 183 °C for 5 min and cooling down for 5 min. Then S1805 (MicroChem, MA, USA) was spin-coated on the LOR 3 A-coated glass wafer in two steps, 500 rpm for 5 seconds and 4000 rpm for 40 seconds, and followed by soft baked at 110 °C for 90 seconds. The wafer was exposed to UV at a dose of 28 mJ/cm<sup>2</sup> using the soft contact/constant dose mode of an EVG 620 mask aligner (EVG, NY, USA), and baked at 110 °C for 60 seconds on a hotplate. The patterned wafer was developed using CD 26 developer (MicroChem, MA, USA) under a base hood for 20 seconds. The developed wafer was cleaned using oxygen plasma etcher at the power of 300 W for 20 seconds. The Ti (25 nm)/Ni (100 nm) was deposited on the patterned wafer using CHA SEC-600 evaporator (CHA Industries, Inc., CA, USA) and placed in PG Remover (MicroChem, MA, USA) solution, warmed at 70 °C on a hotplate, for the lift off process. Each array of  $\mu$ -magnets was cut using Disco DAD-6TM Wafer Dicing Saw (Disco Corporation, Tokyo, Japan) to the size fitting to the microfluidic chip. The PDMS master and glass plate were treated with O<sub>2</sub> plasma using the Diener Electronic Pico oxygen plasma system (Diener Electronic, Ebhausen, Germany) at 50 % power for 2 min, and then an array of  $\mu$ -magnets and a microfluidic channel were aligned and bonded under a microscope.

#### C. DNA preparation

All DNA were purchased from IDTDNA (Coralville, Iowa, USA) and suspended in 10 mM Tris and 1 mM EDTA solution.

#### D. DNA-magnetic particle coupling

The Sera-Mag Carboxylate-Modified Magnetic particles were purchased from GE Health Life Science (Cat # 4415–2105-050,250). The particles were washed two times and suspended in autoclaved DI water at desired concentration before experiment. The 1-Ethyl-3-(dimethylaminopropyl) carbodiimide (EDAC) was purchased from Sigma-Aldrich (St. Louis, MO, USA). To conjugate DNA to bead particles, 100  $\mu$ l of EDAC, 100  $\mu$ l of 500 mM MES (pH 6.0, Bio-world, OH, USA), 100  $\mu$ l of the 10 $\times$ <sup>‡</sup> original stock of the magnetic

particles, 10  $\mu$ L of 100 $\times$ <sup>‡</sup> methylated dsDNA solution, and 690  $\mu$ L of the autoclaved DI water were mixed at 37 °C overnight using a vortex mixer. The mixture suspends 1 $\times$ <sup>‡</sup> DNA (10<sup>11</sup> DNA per  $\mu$ L) conjugated with magnetic particle (1.33 $\times$ 10<sup>7</sup> particle per  $\mu$ L) in 1 % EDAC, 50 mM MES coupling solution. To obtain pure DNA-conjugated beads, multiple washes and incubations were processed. Firstly, the DNA-conjugated beads were washed two times in DI water, two times in 0.1 M Imidazole solution (pH 6.0, Bio-world, OH, USA), and incubated at 37 °C for 5 min. Secondly, the DNA-conjugated beads were washed three times in 0.1 M Sodium Bicarbonate (Fluka-Sigma-Aldrich, MO, USA) and incubated at 37 °C for 5 min. Lastly, the DNA-conjugated beads were washed two times in 0.1 M sodium bicarbonate followed by incubation at 65 °C for 30 min. The N42 permanent magnet was used to hold magnetic particles at the bottom of centrifuge tube while aspirating and adding wash solution. The washed DNA-conjugated particles were re-suspended in 1 $\times$  Tris-EDTA for storage.

**Acknowledgments** The authors would like to acknowledge funding support from National Institute of Health (R21 CA155863), Oxford Nanopore Technologies U.K., and financial support from Mayo-Illinois Alliance for Technology Based Healthcare (<http://mayoillinois.org/>). Finally, authors would like to thank Dr. Gregory Damhorst for experimental advice on qPCR.

#### References

- S. M. Azimi et al., A magnetic bead-based DNA extraction and purification microfluidic device. *Microfluid. Nanofluid.* **11**, 157–165 (2011)
- A. Cerf et al., Single DNA molecule patterning for high-throughput epigenetic mapping. *Anal. Chem.* **83**, 8073–8077 (2011)
- P. M. Das, R. Singal, DNA methylation and cancer. *J. Clin. Oncol. Off. J. Am. Soc. Clin. Oncol.* **22**, 4632–4642 (2004)
- T. P. Forbes, S. P. Forry, Microfluidic magnetophoretic separations of immunomagnetically labeled rare mammalian cells. *Lab Chip* **12**, 1471–1479 (2012)
- L. M. Gonzalez et al., Controlling Magnetotactic Bacteria through an Integrated Nanofabricated Metallic Island And Optical Microscope Approach. *Sci Rep.* **4**, 4104 (2014)
- S. Jahr et al., DNA fragments in the blood plasma of cancer patients: quantitations and evidence for their origin from apoptotic and necrotic cells. *Cancer Res.* **61**, 1659–1665 (2001)
- R. Kandimalla, A. A. van Tilborg, E. C. Zwarthoff, DNA methylation-based biomarkers in bladder cancer. *Nat Rev Urol* **10**, 327–335 (2013)
- K. Kiiantsa, N. Maizels, Ultrasensitive isolation, identification and quantification of DNA-protein adducts by ELISA-Based RADAR assay. *Nucleic Acids Res.* **42**, e108 (2014)
- J. B. Kisiel et al., Stool DNA testing for the detection of pancreatic cancer assessment of methylation marker candidates. *Cancer* **118**, 2623–2631 (2012)
- P. W. Laird, The power and the promise of DNA methylation markers. *Nat. Rev. Cancer* **3**, 253–266 (2003)
- R. Mariella Jr., Sample preparation: the weak link in microfluidics-based biodetection. *Biomed. Microdevices* **10**, 777–784 (2008)

- A. Murrell, V. K. Rakyan, S. Beck, From genome to epigenome. *Hum. Mol. Genet.* **14**, R3–R10 (2005)
- B. Nagy, Z. Ban, Z. Papp, The DNA isolation method has effect on allele drop-out and on the results of fluorescent PCR and DNA fragment analysis. *Clin. Chim. Acta* **360**, 128–132 (2005)
- A. Niemz, T. M. Ferguson, D. S. Boyle, Point-of-care nucleic acid testing for infectious diseases. *Trends Biotechnol.* **29**, 240–250 (2011)
- J. A. Osborn, Demagnetizing factors of the General Ellipsoid. *Phys. Rev.* **67**, 351–357 (1945)
- L. A. Sasso et al., Automated microfluidic processing platform for multiplexed magnetic bead immunoassays. *Microfluid. Nanofluid.* **13**, 603–612 (2012)
- J. C. Sheehan, G. L. Boshart, P. A. Cruickshank, Convenient Synthesis of Water-Soluble Carbodiimides. *J Org Chem* **26**, 2525–2528 (1961)
- J. Shim et al., Detection and quantification of methylation in DNA using solid-state nanopores. *Scientific Reports* **3**, 1389 (2013)
- J. Shim et al., Nanopore-based assay for detection of methylation in double-stranded DNA fragments. *ACS Nano* **9**, 290–300 (2015)
- M. M. Sirdah, Superparamagnetic-bead based method: An effective DNA Extraction from dried blood spots (DBS) for diagnostic PCR. *Journal of clinical and diagnostic research: JCDR* **8**, FC01–FC04 (2014)
- H. W. Wu et al., An integrated microfluidic system for isolation, counting, and sorting of hematopoietic stem cells. *Biomicrofluidics* **4**(2), 024112 (2010)
- H. Z. Zou et al., High detection rates of colorectal neoplasia by stool DNA Testing with a novel digital melt curve assay. *Gastroenterology* **136**, 459–470 (2009)

## Notes

‡ indicates Electric Supplementary Information (ESI) including extra figures and table. DNA and particle concentration Table S1 is included in the ESI.